10166 *Inorg. Chem.* **2010**, *49*, 10166–10173
DOI: 10.1021/ic1014384

Inorganic Chemistry
Article

Assembly of Robust and Porous Hydrogen-Bonded Coordination Frameworks: Isomorphism, Polymorphism, and Selective Adsorption

Ji-Jun Jiang,[†] Mei Pan,[†] Jun-Min Liu,[†] Wei Wang,[‡] and Cheng-Yong Su*[,†]

[†]*MOE Laboratory of Bioinorganic and Synthetic Chemistry, State Key Laboratory of Optoelectronic Materials and Technologies, School of Chemistry and Chemical Engineering, Sun Yat-Sen University, Guangzhou 510275, China, and* [‡]*State Key Laboratory of Applied Organic Chemistry, Lanzhou University, Lanzhou 730000, China*

Received July 19, 2010

By using the tripodal ligand ntb (tris(benzimidazole-2-ylmethyl)amine) and lanthanide nitrate, three isomorphous series of coordination frameworks of the general formula $[Ln(ntb)(NO_3)_3]\cdot$solvents (series **1**: monoclinic *C*2/*c*, Ln = Gd^{3+} and Yb^{3+}; series **2**: hexagonal $P3_1/c$, Ln = Nd^{3+}, Eu^{3+}, Gd^{3+}, and Er^{3+}; series **3**, cubic $Pa\bar{3}$, Ln = Gd^{3+} and Er^{3+}; solvent = H_2O or CH_3OH) have been assembled and characterized with IR, elemental analyses, and single crystal and powder X-ray diffraction methods. In all isomorphous complexes, analogous $[Ln(ntb)(NO_3)_3]$ coordination monomers of the same structure act as the building blocks to be assembled via hydrogen bonds into three-dimensional (3D) frameworks. So the complexes of the same lanthanide ion (for example, the Gd^{3+} ion) from three isomorphous series form polymorphs, for example, monoclinic polymorph **1-Gd**, hexagonal polymorph **2-Gd**, and cubic polymorph **3-Gd**. The single-crystal analyses revealed that the polymorphism was related to different fashions of hydrogen bonding interactions, which was caused by different crystallization conditions, leading to the formation of different 3D hydrogen-bonded frameworks showing distinct porous and topological structures. The monoclinic and hexagonal crystals contain 1D channels, while the cubic crystal is nonporous. The thermogravimetric analyses indicated that all polymorphic crystals have high thermal stability against the removal of guest molecules, and the robust porosity of the hexagonal crystals has been verified by temperature-dependent single-crystal-to-single-crystal measurements upon guest removal/uptake. The solvents adsorption study disclosed that the porous frameworks show high selectivity of benzene against toluene and xylene, while the gas adsorption measurements indicated a moderate H_2, CO_2, and MeOH storage capacity in contrast to low N_2 uptake. The solid-state photoluminescence of the Eu^{3+} and Nd^{3+} complexes in the near-infrared and visible region has also been investigated, offering examples with optical properties tunable by means of isomorphous replacement.

Introduction

The design and synthesis of periodically well-ordered one-, two-, or three-dimensional (1D, 2D, or 3D) coordination frameworks has been an attractive topic in the field of crystal engineering over the past few decades, not only due to their intriguing diversification of structures and topologies but also due to their potential applications in optics, magnetics, catalysis, sensors, and host−guest systems.[1,2] Among these, coordination frameworks with highly stable porous structures are of particular interest because they have shown a brilliant perspective in the application of selective adsorption and gas storage or separation.[3]

*To whom correspondence should be addressed. E-mail: cesscy@mail.sysu.edu.cn.

(1) (a) Férey, G. *Chem. Soc. Rev.* **2008**, *37*, 191. (b) Kitagawa, S.; Kitaura, R.; Noro, S.-i. *Angew. Chem., Int. Ed.* **2004**, *43*, 2334. (c) Janiak, C. *Dalton Trans.* **2003**, 2781. (d) Bradshaw, D.; Claridge, J. B.; Cussen, E. J.; Prior, T. J.; Rosseinsky, M. J. *Acc. Chem. Res.* **2005**, *38*, 273. (e) Eddaoudi, M.; Moler, D. B.; Li, H.-L.; Chen, B.-L.; Reineke, T. M.; O'Keeffe, M.; Yaghi, O. M. *Acc. Chem. Res.* **2001**, *34*, 319. (f) Suh, M. P.; Cheon, Y. E.; Lee, E. Y. *Coord. Chem. Rev.* **2008**, *252*, 1007. (g) Chen, C.-L.; Kang, B.-S.; Su, C.-Y. *Aust. J. Chem.* **2006**, *59*, 3.

(2) (a) Yaghi, O. M.; Li, H.; Davis, C.; Richardardson, D.; Groy, T. L. *Acc. Chem. Res.* **1998**, *31*, 474. (b) Long, D. L.; Hill, R. J.; Blake, A. J.; Champness, N. R.; Hubberstey, P. C.; Schröder, W. M. *Chem.—Eur. J.* **2005**, *11*, 1384. (c) Pan, L.; Olson, D. H.; Ciemnolonski, L. R.; Heddy, R.; Li, J. *Angew. Chem., Int. Ed.* **2006**, *45*, 616. (d) Coronado, E.; Galán-Mascarós, J. R.; Gómez-Garcia, C. J.; Laukhin, V. *Nature* **2000**, *408*, 447. (e) Lacroix, P. G.; Malfant, I.; Benard, S.; Yu, P.; Riviere, E.; Nakatani, K. *Chem. Mater.* **2001**, *13*, 441. (f) Karasawa, S. Y.; Akita; Sano, T.; Koga, N.; Itoh, T.; Iwamura, H.; Rabu, P.; Drilion, M. *J. Am. Chem. Soc.* **1998**, *120*, 10080. (g) Huang, X.-C.; Lin, Y.-Y.; Zhang, J.-P.; Chen, X.-M. *Angew. Chem., Int. Ed.* **2006**, *45*, 1557.

(3) (a) Li, K.; Olson, D. H.; Lee, J. Y.; Bi, W.; Wu, K.; Yuen, T.; Xu, Q.; Li, J. *Adv. Funct. Mater.* **2008**, *18*, 2205. (b) Collins, D. J.; Zhou, H.-C. *Chem. Commun.* **2007**, 3154. (c) Férey, G.; Mellot-Draznieks, C.; Serre, C.; Millange, F. *Acc. Chem. Res.* **2005**, *38*, 217. (d) Kitaura, R.; Seki, K.; Akiyama, G.; Kitagawa, S. *Angew. Chem., Int. Ed.* **2003**, *42*, 428. (e) Hanson, K.; Calin, N.; Bugaris, D.; Scancella, M.; Sevov, S. C. *J. Am. Chem. Soc.* **2004**, *126*, 10502. (f) Dietzel, P. D. C.; Panella, B.; Hirscher, M.; Blom, R.; Fjellvåg, H. *Chem. Commun.* **2006**, 959. (g) Lee, E. Y.; Jang, S. Y.; Suh, M. P. *J. Am. Chem. Soc.* **2005**, *127*, 6374. (h) Beau-vais, L. G.; Shores, M. P.; Long, J. R. *J. Am. Chem. Soc.* **2000**, *122*, 2763. (i) Collins, D. J.; Zhou, H.-C. *J. Mater. Chem.* **2007**, *17*, 3154. (j) Fang, Q.-R.; Zhu, G.-S.; Jin, Z.; Ji, Y.-Y.; Ye, J.-W.; Xue, M.; Yang, H.; Wang, Y.; Qiu, S.-L. *Angew. Chem., Int. Ed.* **2007**, *46*, 6638. (k) Ma, S.; Sun, D.; Simmons, J.; Collier, M. C. D.; Yuan, D.; Zhou, H.-C. *J. Am. Chem. Soc.* **2008**, *130*, 1012.

Published on Web 09/29/2010

Recent research in porous coordination frameworks is mainly focused on the construction of metal−organic frameworks (MOFs) from stiff bridging ligands[1−4] *via* relatively strong dative bonds; nevertheless, the assembly of properly hydrogen-bonded frameworks has been proven to be an alternative approach to getting highly stable porous structures.[5] In principle, there are three possible routes to construct hydrogen-bonded coordination frameworks: (1) self-organizing the discrete coordination modules (zero-dimensional, 0D), which contain both hydrogen bond (HB) donors or acceptors through the formation of complementary HBs into a 3D supramolecular framework (0D → 3D), (2) connecting 1D coordination chains through mutual interchain hydrogen-bonding into a 3D supramolecular framework (1D → 3D), or (3) connecting 2D coordination layers through hydrogen-bonding to a pillared-layer 3D framework (2D → 3D). In this context, the multiple benzimidazole (Bim) derived ligands represent excellent candidates for forming various 0D to 2D coordination motifs ready for hydrogen-bonding into higher dimensional structures due to the following reasons:[6] (a) The Bim groups can be partially or completely deprotonated, leading to versatile coordination and hydrogen-bonding modes. (b) The Bim groups can act both as hydrogen-bonding acceptors and donors, and (c) the Bim groups are apt to form $\pi-\pi$ stacking interactions, which are helpful in stabilizing crystal packing. The hydrogen-bonded frameworks thus generated have also been found to be able to display permanent porosity against guest removal/uptake and show selective guest adsorption behavior.[5a,b]

On the other hand, supramolecular isomerism[7] represents a common phenomenon in the crystal engineering of both hydrogen-bonding and coordination frameworks, which leads to the formation of different structures from the same building blocks. Polymorphism[8] is considered one type of supramolecular isomerism because the same molecular component can generate different supramolecular synthons, therefore giving rise to more than one crystalline form (polymorphs).[7a] In particular, polymorphism exits in molecules which contain multiple hydrogen-bonding moieties, thereby forming multiple supramolecular synthons and/or conformational flexibility.[9] Meanwhile, supramolecular isomorphism also represents a common phenomenon in crystal growth.[10] Isomorphous crystals have the same space group and unit-cell dimensions but only differ in one or more replacement atoms (such as heavy atoms, isomorphous replacement) or additional atoms (such as solvents, isomorphous addition).[11] Typical examples are observed from the assembly of structurally identical frameworks with the same ligands but different metal ions,[10b−d] or exactly identical frameworks containing different guest molecules.[12] In this context, polymorphism and isomorphism can be regarded as two key challenges interrelated in crystal engineering: the former lies at the heart of crystal design and synthetic control, while the latter implies framework versatility and tolerance to active site modification or guest exchange. Therefore, understanding and utilization of polymorphism and isomorphism in crystal engineering may offer opportunities for better physicochemical performance and new product development. The occurrence and relationship of polymorphism

(4) (a) Férey, G.; Mellot-Draznieks, C.; Serre, C.; Millange, F.; Dutour, J.; Surblé, S.; Margiolaki, I. *Science* **2005**, *309*, 2040. (b) Eddaoudi, M.; Kim, J.; Rosi, N.; Vodak, D.; Wachter, J.; O'Keeffe, M.; Yaghi, O. M. *Science* **2002**, *295*, 469. (c) Chui, S. S.-Y.; Lo, S. M.-F.; Charmant, J. P. H.; Orpen, A. G.; Williams, I. D. *Science* **1999**, *283*, 1148.

(5) (a) Lim, S.; Kim, H.; Selvapalam, N.; Kim, K.-J.; Cho, S. J.; Seo, G.; Kim, K. *Angew. Chem., Int. Ed.* **2008**, *47*, 3352. (b) Jiang, J.-J.; Li, L.; Lan, M.-H.; Pan, M.; Eichhöfer, A.; Fenske, D.; Su, C.-Y. *Chem.—Eur. J.* **2010**, *16*, 1841. (c) Malek, N.; Maris, T.; Perron, M.-.; Wuest, J. D. *Angew. Chem., Int. Ed.* **2005**, *44*, 4021. (d) Tanaka, T.; Tasaki, T.; Aoyama, Y. *J. Am. Chem. Soc.* **2002**, *124*, 12453. (e) Kobayashi, K.; Sato, A.; Sakamoto, S.; Yamaguchi, K. *J. Am. Chem. Soc.* **2003**, *125*, 3035. (f) Uemura, K.; Saito, K.; Kitagawa, S.; Kita, H. *J. Am. Chem. Soc.* **2006**, *128*, 16122. (g) Aakeröy, C. B.; Beatty, A. M.; Leinen, D. S. *Angew. Chem., Int. Ed.* **1999**, *38*, 1815. (h) Dalrymple, S. A.; Shimizu, G, K. H. *J. Am. Chem. Soc.* **2007**, *129*, 12114. (i) Stephensonn, M. D.; Hardie, M. J. *CrystEngComm* **2007**, *9*, 496. (j) Beatty, A. M. *Coord. Chem. Rev.* **2003**, *246*, 131.

(6) (a) Su, C. Y.; Yang, X. P.; Kang, B. S.; Mak, T. C. W. *Angew. Chem., Int. Ed.* **2001**, *40*, 1725. (b) Su, C. Y.; Kang, B. S.; Liu, H. Q.; Wang, Q. G.; Mak, T. C. W. *Chem. Commun.* **1998**, 1551. (c) Chen, C.-L.; Tan, H.-Y.; Zhang, Q.; Yao, J.-H.; Su, C.-Y. *Inorg. Chem.* **2005**, *44*, 8510. (d) Chen, C.-L.; Zhang, J.-A.; Li, X.-P.; Chen, Z.-N.; Kang, B.-S.; Su, C.-Y. *Inorg. Chim. Acta* **2005**, *358*, 4527. (e) Su, C. Y.; Kang, B. S.; Yang, Q.-C.; Mak, T. C. W. *J. Chem. Soc., Dalton Trans.* **2000**, 1857. (f) Su, C. Y.; Kang, B. S.; Du, C.-X.; Yang, Q.-C.; Mak, T. C. W. *Inorg. Chem.* **2000**, *39*, 4843. (g) Zheng, S.-R.; Yang, Q.-Y.; Yang, R.; Pan, M.; Cao, R.; Su, C.-Y. *Cryst. Growth Des.* **2009**, *9*, 2341. (h) Liu, Y.-R.; Li, L.; Yang, T.; Yu, X.-W.; Su, C.-Y. *CrystEngComm* **2009**, *11*, 2712. (i) Chen, C.-L.; Zhang, Q.; Yao, J.-H.; Zhang, J.-Y.; Kang, B.-S.; Su, C.-Y. *Inorg. Chim. Acta* **2008**, *361*, 2934. (j) Li, X.-P.; Zhang, J.-Y.; Pan, M.; Zheng, S.-R.; Liu, Y.; Su, C.-Y. *Inorg. Chem.* **2007**, *46*, 4617. (k) Li, X.-P.; Pan, M.; Zheng, S.-R.; Liu, Y.-R.; He, Q.-T.; Kang, B.-S.; Su, C.-Y. *Cryst. Growth Des.* **2007**, *7*, 2481. (l) Su, C.-Y.; Kang, B.-S.; Mu, X.-Q.; Sun, J.; Tong, Y.-X.; Chen, Z.-N. *Aust. J. Chem.* **1998**, *51*, 565.

(7) (a) Moulton, B.; Zaworotko, M. J. *Chem. Rev.* **2001**, *101*, 1629. (b) Zhang, J.-P.; Huang, X.-C.; Chen, X.-M. *Chem. Soc. Rev.* **2009**, *38*, 2385. (c) Lü, X. Q.; Qiao, Y, Q.; He, J. R.; Pan, M.; Kang, B. S.; Su, C. Y. *Cryst. Growth Des.* **2006**, *6*, 1910. (d) Muthu, S.; Yip, J. H. K.; Vittal, J. J. *J. Chem. Soc., Dalton Trans.* **2001**, 3577. (e) MacGillivray, L. R.; Reid, J. L.; Ripmeester, J. A. *Chem. Commun.* **2001**, 1034. (f) Carlucci, L.; Ciani, G.; Proserpio, D. M.; Spadacini, L. *CrystEngComm* **2004**, *6*, 96. (g) Barnett, S. A.; Blake, A. J.; Champness, N. R.; Wilson, C. *Chem. Commun.* **2002**, 1640. (h) Black, A. J.; Brooks, N. R.; Champness, N. R.; Crew, M.; Deveson, A.; Fenske, D.; Greogory, D. H.; Hanton, L. R.; Hubberstey, P.; Schröder, M. *Chem. Commun.* **2001**, 1432. (i) Gao, E. Q.; Wang, Z.-M.; Liao, C.-S.; Yan, C. H. *New J. Chem.* **2002**, *26*, 1096. (j) Shin, D. M.; Lee, I. S.; Chung, Y. K.; Lah, M. S. *Inorg. Chem.* **2003**, *42*, 5459. (k) Lü, X.-Q.; Jiang, J.-J.; zur Loye, H.-C.; Kang, B.-S.; Su, C.-Y. *Inorg. Chem.* **2005**, *44*, 1810. (l) Su, C.-Y.; Goforth, A. M.; Smith, M. D.; zur Loye, H.-C. *Inog. Chem.* **2003**, *42*, 5685. (m) James, S. L. *Macromol. Symp.* **2004**, *209*, 119. (n) Puddephatt, R. J. *Chem. Soc. Rev.* **2008**, *37*, 2012. (o) Zhang, Q.; Zhang, J.; Yu, Q.-Y.; Pan, Me.; Su, C.-Y. *Cryst. Growth Des.* **2010**, *10*, 4076.

(8) (a) McCrone, W. C. Polymorphism. In *Physics and Chemistry of the Organic Solid-State*; Interscience: New York, 1965. (b) Bernstein, J. *Polymorphism in Molecular Crystals*; Oxford University Press: Oxford, U. K., 2002. (c) Threlfall, T. L. *Analyst* **1995**, *120*, 2435. (d) Davey, R. J. *Chem. Commun.* **2003**, 1463. (d) Byrn, S. R.; Pfeiffer, R. R.; Stowell, J. G. *Solid-State Chemistry of Drugs*; SSCI: West Lafayette, IN, 1999. (e) Desiraju, G. R. *Angew. Chem., Int. Ed. Engl.* **1995**, *34*, 2311. (f) Stahly, G. P. *Cryst. Growth Des.* **2007**, *7*, 1007.

(9) (a) Bernstein, J. Conformational Polymorphism. In *Organic Solid State Chemistry*; Desiraju, G. R., Ed.; Elsevier: Amsterdam, 1987; p 471. (b) Bilton, C.; Howard, J. A. K.; Madhavi, N. N. L.; Nangia, A.; Desiraju, G. R.; Allen, F. H.; Wilson, C. C. *Chem. Commun.* **1999**, 1675. (c) Kumar, V. S. S.; Addlagatta, A.; Nangia, A.; Robinson, W. T.; Broder, C. K.; Mondal, R.; Evans, I. R.; Howard, J. A. K.; Allen, F. H. *Angew. Chem., Int. Ed.* **2002**, *41*, 3848.

(10) (a) Mahmoudkhani, A. H.; Langer, V. *Cryst. Growth Des.* **2002**, *2*, 21. (b) MacDonald, J. C.; Luo, T.-J. M.; Palmore, G. T. R. *Cryst. Growth Des.* **2004**, *4*, 1230. (c) Tanase, S.; Andruh, M.; Müller, A.; Schmidtmann, M.; Mathonièrec, C.; Rombaut, G. *Chem. Commun.* **2001**, 1084. (d) Jiang, J.-J.; Li, L.; Yang, T.; Kuang, D.-B.; Wang, W.; Su., C.-Y. *Chem. Commun.* **2009**, 2387. (e) Sethuraman, V.; Stanley, N.; Muthiah, P. T; Sheldrick, W. S.; Winter, M.; Luger, P.; Weber, M. *Cryst. Growth Des.* **2003**, *3*, 823.

(11) (a) Vijayan, M.; Ramaseshan, S. *International Tables for Crystallography*; Springer: New York, 2006; Vol. B, Chapter 2.4, pp 264−275. (b) Klop, E. A.; Krabbendam, H.; Kroon, J. *Acta Crystallogr.* **1987**, *A43*, 810.

(12) (a) Ohmori, O.; Kawano, M.; Fujita, M. *J. Am. Chem. Soc.* **2004**, *126*, 16292. (b) Deiters, E.; Bulach, V.; Hosseini, M. W. *Chem. Commun.* **2005**, 3906. (c) Zhuang, C.-F.; Zhang., J.-Y.; Wang, Q.; Chu, Z.-H.; Fenske, D.; Su, C.-Y. *Chem.—Eur. J.* **2009**, *15*, 7578. (d) Wang, Q.; Zhang, J.-Y.; Zhuang, C.-F.; Tang, Y.; Su, C.-Y. *Inorg. Chem.* **2009**, *48*, 287.

Scheme 1. Schematic Representation for 0D → 3D Hydrogen-Bonding Assembly from the [Ln(ntb)$(NO_3)_3$] Building Modules[a]

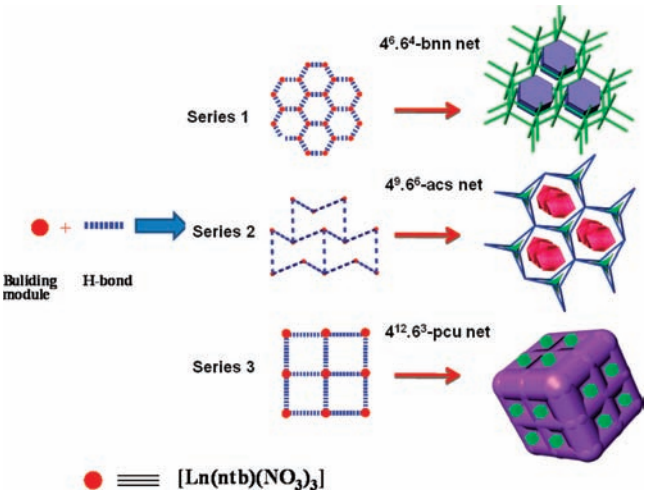

[a] The filling space indicates the solvent-accessible voids.

and isomorphism have been thoroughly investigated and well understood in pharmaceutical and inorganic solid-state chemistry;[13] however, few little attention has been paid to the crystal engineering of porous hydrogen-bonding and coordination frameworks.[14]

We have previously observed two crystal structures from the reaction of a tripodal ligand tris-(benzimidazole-2-ylmethyl)amine (ntb) and lanthanide nitrates, which showed the same coordination motifs but a distinct symmetry and space group.[6l] Herein, we report a systematic study of this reaction, which offered three series of hydrogen-bonded coordination networks, namely, $\{[Ln(ntb)(NO_3)_3]\cdot xH_2O\}_n$ (series **1**: monoclinic $C2/c$, Ln = Gd and Yb; series **2**: hexagonal $P3_1/c$, Ln = Eu, Gd, Er and Nd; x = 0−3) or $\{[Ln(ntb)(NO_3)_3]\cdot 1.5CH_3OH\}_n$ (series **3**: cubic $Pa\bar{3}$, Ln = Gd and Er). Concomitant isomorphism and polymorphism was studied with respect to crystallization conditions and hydrogen-bonding fashions. As shown in Scheme 1, the same coordination subunits [Ln(ntb)$(NO_3)_3$] were found to be consolidated by HBs in different ways: N−H···O and O−H···O hydrogen-bonded in series **1** to give monoclinic frameworks, while N−H···O HBs dominated in series **2** and **3** to form hexagonal and cubic frameworks, respectively. Although all three series complexes all feature high thermal stability, the hexagonal series display distinctive porosity and robustness against water removal/uptake and show selective solvent and gas adsorption properties. The thermal stability and guest adsorption/desorption behaviors have also been investigated by thermal gravimetric analysis (TGA) and powder X-ray diffraction (XRD).

Result and Discussion

Syntheses, Polymorphism, and Isomorphism. All of the complexes are readily available by direct reaction of the

Scheme 2. Schematic Representation for the Structure of the Ligand and the Formation of the Three Series Complexes

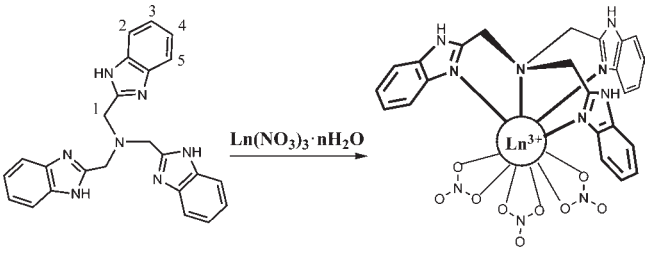

1) monoclinic series: 1-Gd·$2H_2O$, 1-Yb·$2H_2O$
2) hexagonal series: 2-Eu, 2-Gd, 2-Gd·$2H_2O$, 2-Er·H_2O, 2-Nd·$3H_2O$
3) cubic series: 3-Gd·$1.5CH_3OH$, 3-Er·$1.5CH_3OH$

hydrated lanthanide nitrate $Ln(NO_3)_3\cdot 6H_2O$ with the ntb ligand, offering the same monomeric [Ln(ntb)$(NO_3)_3$] coordination motif as shown in Scheme 2. However, polymorphous crystals were formed depending on the reaction systems. Upon the diffusion of diethyl ether into CH_3OH solution, the crystals were crystallized in a monoclinic system with the space group $C2/c$ (**1-Gd·$2H_2O$** and **1-Yb·$2H_2O$**), while upon the diffusion of diethyl ether into the CH_3OH−DMF (v:v = 2:1) mixture, the crystals were crystallized in a hexagonal system with the space group $P3_1/c$ (**2-Eu**, **2-Gd·$2H_2O$**, **2-Er·H_2O**, and **2-Nd·$3H_2O$**). Interestingly, when changing the ratio of the CH_3OH−DMF mixture to v/v = 4:1, the crystals were crystallized in a cubic system with the space group $Pa\bar{3}$ (**3-Gd·$1.5CH_3OH$** and **3-Er·$1.5CH_3OH$**). All complexes have been characterized by elemental analyses and IR spectra. The phase purity of the bulk samples has been checked using powder XRD, which shows that the measured patterns are in agreement with the simulated ones from the single-crystal diffraction data (Figures S1−3, Supporting Information).

It is evident that the solvents used for crystallization play an important role in the formation of crystal polymorphs. The DMF, CH_3OH, and H_2O (coming from hydrated salts and a trace impurity of DMF and CH_3OH) solvent molecules were selectively crystallized with [Ln(ntb)-$(NO_3)_3$] coordination monomers to result in crystals of different symmetry, of which the DMF solvent seems only to influence the crystallization process but not participate in crystallization. For each crystal polymorph, complexes of different lanthanide ions were prepared to form isomorphous series. That is, monoclinic series **1-Gd·$2H_2O$** and **1-Yb·$2H_2O$**; hexagonal series **2-Eu**, **2-Gd·$2H_2O$**, **2-Er·H_2O**, and **2-Nd·$3H_2O$**; and cubic series **3-Gd·$1.5CH_3OH$** and **3-Er·$1.5CH_3OH$**. In each series, complexes only differ in metal atoms (isomorphous replacement) or solvent atoms (isomorphous addition)[11] but retain the same space group and unit-cell dimensions. Strictly speaking, only the complexes having the same lanthanide ion and solvent molecules from three isomorphous series can be called polymorphs, like **1-Gd·$2H_2O$** and **2-Gd·$2H_2O$**. However, since the corresponding [Ln(ntb)$(NO_3)_3$] coordination monomers in the three series are exactly the same and solvent molecules could be removed without changing the crystal lattice, complex **3-Gd·$1.5CH_3OH$** may also be considered as a polymorph with **1-Gd·$2H_2O$** and **2-Gd·$2H_2O$** in a supramolecular sense.[7] Indeed, the water and methanol molecules in **1-Gd·$2H_2O$**, **2-Gd·$2H_2O$**, and **3-Gd·$1.5CH_3OH$** crystals can slowly escape, partially, when left in the open air and can be completely removed at elevated temperatures to lead to **1-Gd**,

(13) (a) Brittain, H. G. *J. Pharm. Sci.* **2007**, *96*, 705. (b) Desiraju, G. R. *Cryst. Growth Des.* **2008**, *8*, 3. (c) Zencirci, N.; Gelbrich, T.; Kahlenberg, V.; Griesser, U. J. *Cryst. Growth Des.* **2009**, *9*, 3444. (d) Zwijnenburg, M. A.; Cora, F.; Bell, R. G. *J. Am. Chem. Soc.* **2008**, *130*, 11082.

(14) (a) Jiang, J.-J.; Zheng, S.-R.; Liu, Y.; Pan, M.; Wang, W.; Su., C.-Y. *Inorg. Chem.* **2008**, *47*, 10692. (b) Kanoo, P.; Gurunatha, K. L.; Maji, T. K. *Cryst. Growth Des.* **2009**, *9*, 4147.

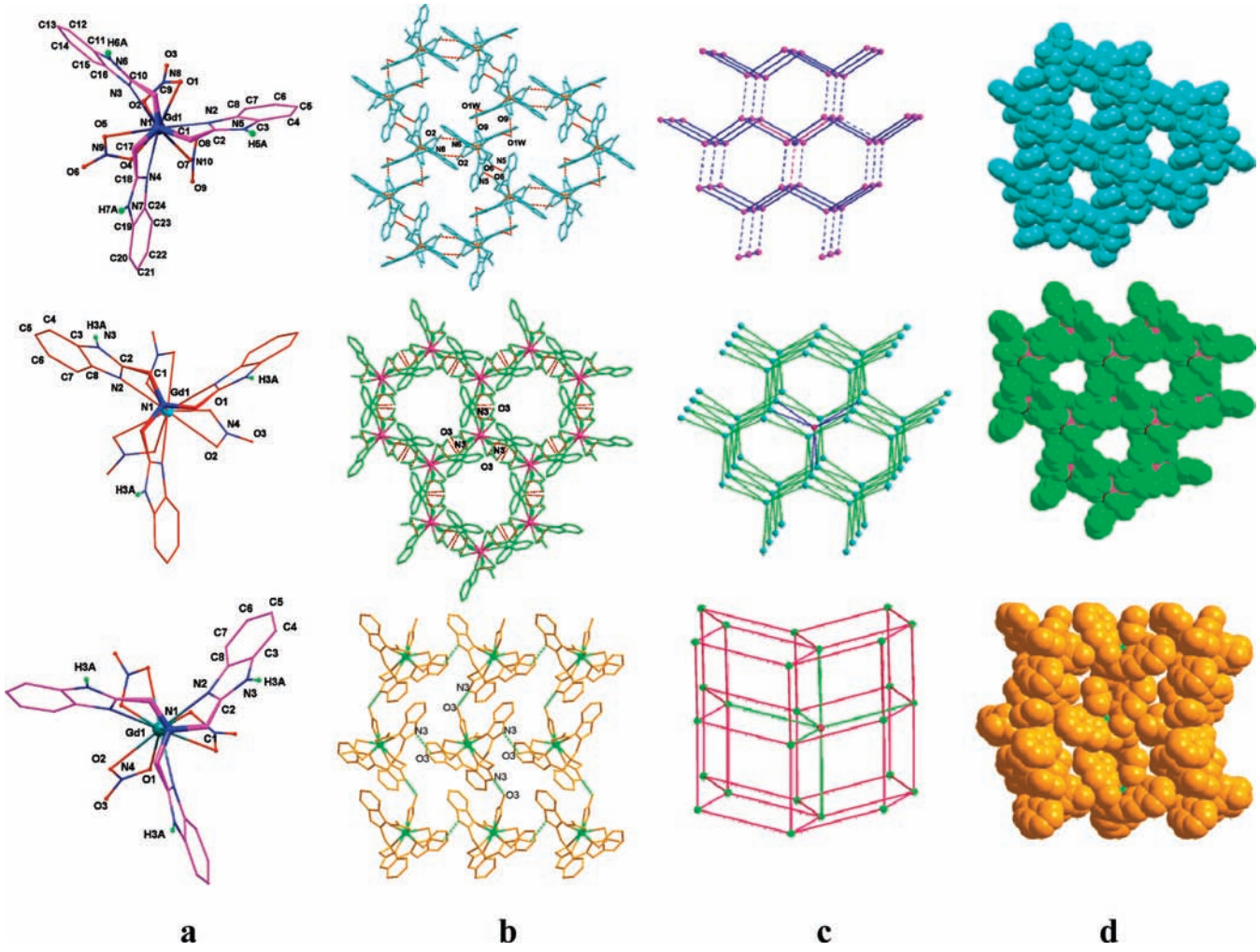

Figure 1. Crystal structures of complexes **1-Gd·2H$_2$O** (upper), **2Gd·2H$_2$O** (middle), and **3-Gd·1.5CH$_3$OH** (lower). (a) Molecular structures showing the coordination geometry of the Gd^{3+} ion in [Gd(ntb)(NO$_3$)$_3$] motifs; (b) 2D layers formed by hydrogen-bonding shown in dashed lines; (c) 3D frameworks sustained by hydrogen bonds between 2D layers showing the packing fashion and net topology; (d) 1D channels or lattice cavities formed in 3D hydrogen-bonding frameworks shown in the space-filling mode (guest molecules are omitted for clarity).

2-Gd, and **3-Gd**, which have the same single crystal nature as their solvated analogues (vide infra). The appearance of concomitant polymorphism and isomorphism in these complexes suggests that each polymorph as a structural model can be expanded into isomorphous series by modifying or replacing building units, while every isomorph as a specific compound may be able to turn into a desired polymorphous structure by controlling the crystallization conditions. This provides good chances to tune structures suitably for required properties in crystal engineering.

Crystal Structures and Hydrogen-Bonding Frameworks. The single-crystal data of all complexes have been collected and summarized in Tables S1 and S2 (Supporting Information). As representatives of three isomorphous series, **1-Gd·2H$_2$O**, **2-Gd·2H$_2$O**, and **3-Gd·1.5CH$_3$OH** are selected for discussion. In general, the central Gd^{3+} ion is 10-coordinated by four N atoms from the tetradentate ntb ligand and six O atoms from three nitrate groups, as shown in Figure 1a, giving rise to the same [Gd(ntb)(NO$_3$)$_3$] coordination unit. The ligand ntb exhibits a tripodal coordination fashion with three benzimidazole (Bim) arms forming a propeller host to catch hold of the central Gd^{3+} ion, leaving three NH groups on one side as HB donors and nine O atoms from three nitrate groups on the other side as HB acceptors. Selected bond lengths and angles are listed in Tables S3−S5 (Supporting Information). We can see that the Gd−N and Gd−O distances in **1-Gd·2H$_2$O**, **2-Gd·2H$_2$O**, and **3-Gd·1.5CH$_3$OH** are comparable, regardless of the packing fashions of the [Gd(ntb)(NO$_3$)$_3$] motifs in different polymorphs.

The crystal packing analyses disclosed that HBs play crucial roles in directing arrangements of the [Gd(ntb)(NO$_3$)$_3$] building units in the crystal lattice of three complexes. In principle, each [Gd(ntb)(NO$_3$)$_3$] unit can provide three −NH HB donors and nine O HB acceptors. As depicted in Figures 1b and S4a (Supporting Information), each [Gd(ntb)(NO$_3$)$_3$] unit in **1-Gd·2H$_2$O** forms three crystallographically unique N−H···O HBs (N(6)···O(3), 2.80 Å, ∠NHO, 159°; N(5)···O(6), 2.94 Å, ∠NHO, 166°; N(7)···O1W, 2.85 Å, ∠NHO, 146°) and one O−H···O HB (O(9)···O1w, 2.79 Å) (Table S5, Supporting Information). In the *ab* plane, these HBs link side-by-side neighboring [Gd(ntb)(NO$_3$)$_3$] units alternately in the opposite direction to generate a honeycomb 6^3 2D layer, where intermolecular $\pi\cdots\pi$ interactions (3.71 Å) are present between adjacent Bim rings. In addition, the

N(6)···O(3) HBs join such 2D layers along the *c* axis, causing an overlapped crystal packing of the 6^3 2D layers as depicted in Figure S4b (Supporting Information). If considering every [Gd(ntb)$(NO_3)_3$] unit as a connecting node, a 5-connected **bnn**-type 3D hydrogen-bonding framework is generated, as simplified in Figure 1c, showing a net topology of point symbol $4^6.6^4$ (Scheme 1), which is rarely observed.[15]

By contrast, in **2-Gd·2H$_2$O**, every [Gd(ntb)$(NO_3)_3$] unit forms two sets of crystallographically equivalent N−H···O HBs (N(3)···O(3), 3.02 Å, ∠NHO, 128°; N(3)···O(2), 2.99 Å, ∠NHO, 163°) with six different neighboring [Gd(ntb)$(NO_3)_3$] units (Figure S4a, Supporting Information). Each set of HBs joins adjacent [Gd(ntb)$(NO_3)_3$] units into a double layer extending in the *ab* plane (Figure 1b). If we consider such a double layer also as a honeycomb 6^3 2D network analogous to that in **1-Gd·2H$_2$O**, an offset crystal packing of double layers along the *c* axis is obvious, as seen in Figure S4b (Supporting Information). Therefore, alternate stacking of such double layers is sustained by the second set of N−H···O HBs to generate a 6-connected **acs**-type 3D framework, as simplified in Figure 1c, giving a net topology of point symbol $4^9.6^6$ (Scheme 1), which is also uncommon.[16]

Similar to those in **2-Gd·2H$_2$O**, complex **3-Gd·1.5CH$_3$OH** also forms six N−H···O HBs (N(3)···O(3), 2.94 Å, ∠NHO, 133°), as shown in Figure S4a (Supporting Information). However, the high crystal symmetry makes these six HBs crystallographically equivalent, thus resulting in a completely different crystal packing fashion, in contrast to that of the **2-Gd·2H$_2$O** complex. For a comparison, four N−H···O HBs in the *ab* plane connect four different [Gd(ntb)$(NO_3)_3$] neighbors to form a 2D waving layer, as depicted in Figures 1b and S4b (Supporting Information). If considering such waving layers as 4^4 grids, a slightly offset crystal packing of these grids is consolidated by the remaining two N−H···O HBs along the *c* axis. Therefore, a 6-connected **pcu**-type 3D framework is generated, as simplified in Figure 1c, showing a net topology of point symbol $4^{12}.6^3$ (Scheme 1), which is quite common.[6b,e]

From the above discussion, we can see that, overall, 3D hydrogen-bonded coordination frameworks are constructed in **1-Gd·2H$_2$O**, **2-Gd·2H$_2$O**, and **3-Gd·1.5CH$_3$OH**, and a two-step 0D → 3D assembly process can be outlined from the complementary HB self-organizing of the discrete coordination modules [Ln(ntb)$(NO_3)_3$], which contain both HB donors and acceptors (Scheme 1). However, crystallization under a different solvent system caused the formation of distinct HBs, which in turn direct the crystal packing fashion of the same [Ln(ntb)$(NO_3)_3$] building units, leading to three types of crystal polymorphs. In **1-Gd·2H$_2$O**, the overlapped stacking of the 6^3 2D layers results in a monoclinic framework which offers 1D cylindrical channels encircled by six Bim rings with an effective pore diameter of 4.0 Å (separation between two closest opposite atoms after considering van der Waals radii) in the *c* direction (Figure 1d). In **2-Gd·2H$_2$O**, the offset packing of the 6^3 2D double layers gives rise to a hexagonal framework which offers 1D triangular channels encompassed by three Bim rings with an effective pore diameter of 5.0 Å in the *c* direction (Figure 1d). However, in **3-Gd·1.5CH$_3$OH**, the slightly offset stacking of the 4^4 2D grid layers leads to a cubic framework which contains lattice cavities hosting CH_3OH guests but no obvious channels. There are windows in the *a*, *b*, and *c* directions for the escape of guest molecules, but they are too narrow to release guests easily (Scheme 1). The guest water or methanol molecules are encapsulated inside these channels or cavities, which account for 21.1% in **1-Gd,** 28.5% in **2-Gd**, and 15.3% in **3-Gd** of the potential solvent accessible area, as calculated by PLATON.[17] Therefore, these polymorphs present an interesting example that crystal porosity can be finely tuned by changing crystal forms. In other words, modification of crystal porosity can be achieved through the formation of a series of polymorph crystals of the same building modules.

Thermal Stability and Single-Crystal-to-Single-Crystal De/Rehydration. Thermal gravimetric analyses (TGA) were performed to examine the thermal stability of three polymorphous crystals (Figure S5, Supporting Information). TGA curves were recorded for the freshly prepared bulk samples of **1-Gd·2H$_2$O**, **1-Yb·2H$_2$O**, **2-Gd·2H$_2$O**, **3-Gd·1.5CH$_3$OH**, and **3-Er·1.5CH$_3$OH** in the temperature range 25−700 °C. A long slope observed in **1-Gd·2H$_2$O** and **1-Yb·2H$_2$O** indicated that all water molecules were removed before 200 °C, giving weight losses of 3.4 and 4.4% (cal. 4.6 and 4.5%), respectively. The frameworks started to decompose at about 280 for **1-Gd·2H$_2$O** and 300 °C for **1-Yb·2H$_2$O**, where an abrupt weight loss occurred. For **3-Gd·1.5CH$_3$OH** and **3-Er·1.5CH$_3$OH**, an even slower procedure of guest molecule escape was observed, which lasted to about 290 °C, corresponding to weight losses of 5.4 and 4.2% for methanol molecules (calcd 6.0 and 5.9%). The frameworks began to collapse at about 300 °C. By contrast, the TGA behaviors of the monoclinic polymorph look quite different. Complex **2-Gd·2H$_2$O** displayed a rapid weight loss before 100 °C (3.6%), and then followed with a second loss between 100 and 150 °C (1.2%), totally amounting to two water molecules per Gd^{3+} (calcd 4.6%). To check whether water solvents are completely evacuated, the dehydrated sample **2-Gd** was measured once more. As shown in Figure S5b (Supporting Information), there was no obvious weight loss before 280 °C.

Since TGA investigation can only provide the thermal stability and desolvation behavior of crystals without providing convincing information on the integrity of the framework at elevated temperatures, the single-crystal-to-single-crystal re/dehydration was carried out for the same polymorphous crystals, which provided conclusive evidence of the robustness for the hydrogen-bonded coordination frameworks against guest evacuation. After collecting reflection data on a single crystal of **2-Gd·2H$_2$O**, the same crystal was *in situ* heated to 200 °C (473 K) and then cooled down in the air to 20 °C (293 K). The single crystallinity was found to be retained during variable temperature measurements, and the corresponding reflecting data were collected, assigning **2-Gd** (473 K) and **2-Gd·H$_2$O** (473K-air), respectively, in Tables S1 and S2 (Supporting Information). The structural analyses

(15) Pan, L.; Ching, N.; Huang, X.-Y.; Li, J. *Chem. Commun.* **2001**, 1064.
(16) Sudik, A. C.; Cote, A. P.; Yaghi, O. M. *Inorg. Chem.* **2005**, *44*, 2998.
(17) Spek, A. L. *J. Appl. Crystallogr.* **2003**, *36*, 7.

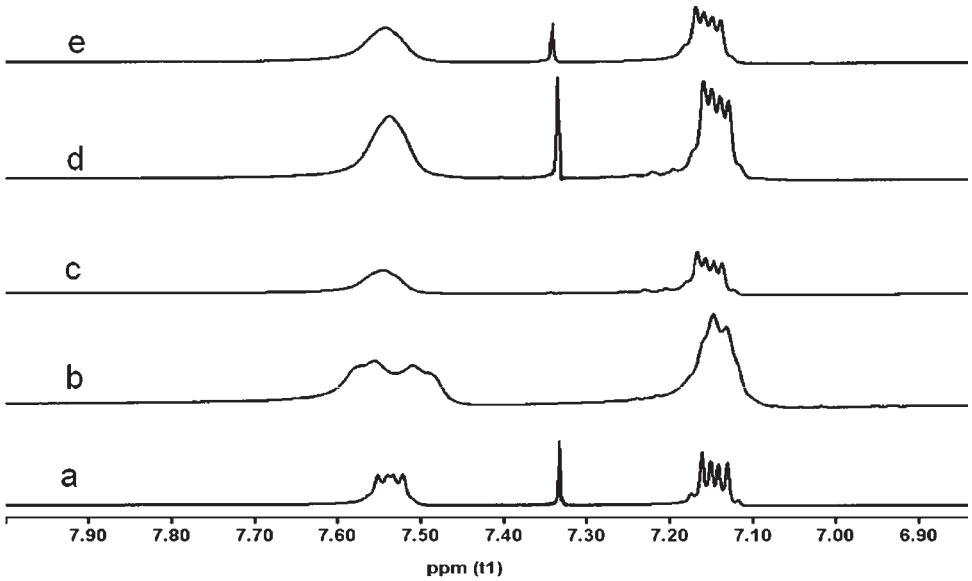

Figure 2. H^1 NMR spectra of **2-Gd** after (a) dipping in benzene, (b) dipping in toluene, (c) dipping in dimethylbenzene, (d) dipping in a benzene/toluene mixture (v/v = 1:1), and (e) dipping in a benzene/dimethylbenzene mixture (v/v = 1:1).

confirmed that the $[Gd(ntb)(NO_3)_3]$ coordination motifs and their overall crystal packing fashions remained almost intact after heating. However, the guest water molecules inside the channels have been completely removed at 200 °C, evidenced by the small electron residua of 0.58 e $Å^{-3}$ in the final refinement of **2-Gd** (473 K). Upon cooling the completely dehydrated crystal from 200 to 20 °C in the air, one water molecule per Gd^{3+} was rehydrated, which has been verified by the satisfactory refinement of the data set from **2-Gd·H_2O** (473 K-air) and is consistent with the TGA results discussed above. Similarly, unit-cell checking of the dehydrated crystals of **1-Gd** and **3-Gd** also verified that the crystal space groups and cell dimensions showed little change after heating, indicating that the hydrogen-bonding frameworks were retained after the removal of guest molecules.

Solvent and Gas Adsorption. The sample of dehydrated **2-Gd** has been tested for solvent guest adsorption according to the following procedure: (1) Dry the sample at 180 °C under a vacuum for 12 h. (2) Dip the dehydrated sample into solvents for 72 h. (3) Filter out and wash the dipped sample with anhydrous ethyl ether three times, and then dry it in an infrared oven for 12 h. (4) Carry out ^1H NMR measurements. The following solvent systems have been selected: (1) benzene, (2) toluene, (3) dimethylbenzene, (4) benzene and toluene (v/v = 50:50), and (5) benzene and dimethylbenzene (v/v = 50:50). As shown in Figure 2, ^1H NMR monitoring shows that only benzene molecules can be adsorbed as guests. Toluene and dimethylbenzene molecules could not be adsorbed in either pure solvents or mixtures, indicative of a high selectivity of benzene over its derivatives by porous **2-Gd**. Such guest adsorption selectivity may be due to the size effect of the 1D pores in **2-Gd**, implying potential utilizations in separation, or detection, cleaning, and protection in environmental applications.[3]

To evaluate the permanent porosity of the open framework in **2-Gd** and to estimate its possible application for gas separation or storage, gas and vapor adsorption behaviors have been investigated with N_2, CO_2, H_2, and MeOH. The as-synthesized samples (weight 50−100 mg) were dried under a high vacuum at 120 °C for 24 h to remove water molecules prior to measurements. The adsorption isotherms of N_2 measured at 77 K for **2-Gd** indicate that only surface adsorption has occurred, suggesting that nitrogen molecules cannot diffuse into the channels at this temperature. In contrast, the adsorption isotherms of CO_2 measured at 195 K exhibit type-I like profiles, as shown in Figure 3a. Analysis of the results discloses that **2-Gd** has a CO_2 adsorption capacity of 70.2 mL g^{-1}, amounting to 2.4 CO_2 molecules per metal ion, significantly larger than analogous Sm^{3+} complexes reported before.[5b] Such adsorption selectivity of CO_2 over N_2 may be due to the fact that CO_2 molecules have a larger quadrupole moment than N_2, which has a smaller molecular size (CO_2 3.4, N_2 3.1 Å) but bigger kinetic diameters (CO_2 3.3, N_2 3.6 Å). Improving the CO_2/N_2 selectivity is always expected for a promising outcome of the separation of CO_2 from natural gas and flue gas by porous materials. The high-pressure (up to 100 bar) hydrogen storage capability was evaluated at 77 K. The result indicates that **2-Gd** possesses a comparable capacity of H_2 storage to that of Sm^{3+} analogues, reaching 0.73% and corresponding to 2.7 H_2 molecules per metal ion (Figure 3b). The isotherm is approximately linear, suggesting that porous **2-Gd** is possibly undersaturated with H_2 in the pressure range explored.[18] As shown in Figure 3c, the adsorption isotherms of MeOH vapor measured at 298 K revealed a maximum storage amount of 147.1 mg g^{-1} for MeOH at 1 atm, corresponding to 3.5 MeOH molecules per metal ion.

Photophysical Properties. The solid-state photoluminescence spectra for complex **2-Eu** were recorded at room temperature. As shown in Figure S6a (Supporting Information), **2-Eu** shows salient emission peaks at 592, 613, and 622 nm which are attributed to $^5D_0 \rightarrow {}^7F_1$ and $^5D_0 \rightarrow {}^7F_2$ transitions, with the former being a magnetic

(18) Rosi, N. L.; Eckert, J.; Eddaoudi, M.; Vodak, D. T.; Kim, J.; O'Keeffe, M.; Yaghi, O. M. *Science* **2003**, *300*, 1127.

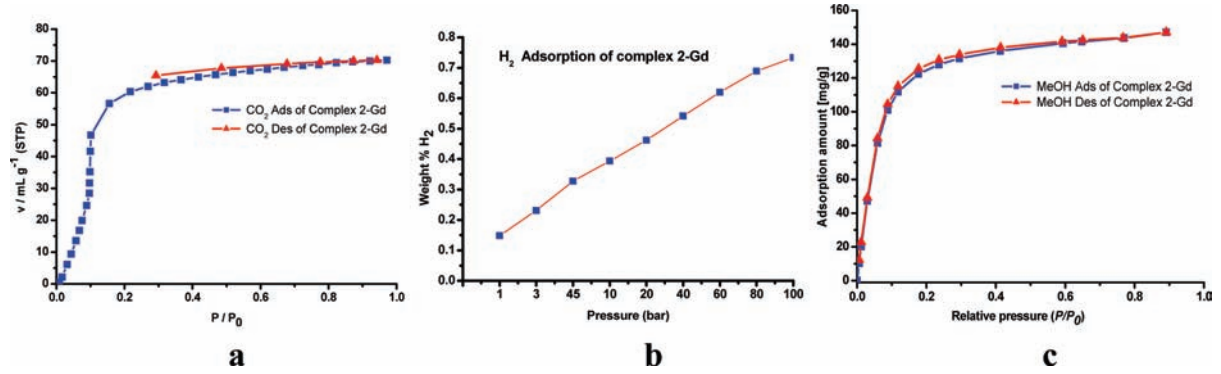

Figure 3. (a) CO_2 adsorption/desorption isotherms at 195 K for **2-Gd**. (b) H_2 adsorption properties of **2-Gd** at 77 K. (c) MeOH sorption isotherms of **2-Gd** measured at 298 K. P_0 is the saturation pressure (MeOH 16.94 kPa), and the samples were activated at 120 °C for 24 h.

dipole allowed transition (MD) and the latter belonging to an electric induced dipole transition (ED). The splittings of the peaks can be deciphered from the slightly different coordination of Eu^{3+} in the solid state. It is well know that the Eu^{3+} luminescent transitions of $^5D_0 \rightarrow {}^7F_1$ and $^5D_0 \rightarrow {}^7F_2$ can be theoretically used to identify its coordination sphere and symmetry environment. In general, when the Eu^{3+} ion is positioned in a higher-symmetry environment containing an inversion center, the $^5D_0 \rightarrow {}^7F_1$ transition is predominant, while in a lower-symmetry environment without an inversion center, the $^5D_0 \rightarrow {}^7F_2$ transition becomes stronger. The comparison of the intensity between both peaks of 611 and 592 nm obviously shows that the $^5D_0 \rightarrow {}^7F_2$ transition is stronger than the $^5D_0 \rightarrow {}^7F_1$ transition, which indicates that the Eu^{3+} ion lies in a noncentrosymmetric coordination site in the solid state,[19a] in agreement with single-crystal structural analysis results. A small peak at 580 nm is noticeable, which can be assigned to the $^5D_0 \rightarrow {}^7F_0$ transition originating from a first-order perturbation strictly forbidden transition, according to Judd–Ofelt theory.[19b] The total emission spectra in the NIR region were recorded from 800−1500 nm for **2-Nd·3H$_2$O**. Figure S6b (Supporting Information) shows emission peaks at 920 and 1060 nm which are attributed to $^4F_{3/2} \rightarrow {}^4I_{9/2}$ and $^4F_{3/2} \rightarrow {}^4I_{11/2}$ transitions of the Nd^{3+} ion. These observation indicate that the energy transfer can take place, but weakly. Since **2-Eu** and **2-Nd·3H$_2$O** are isomorphous structures, they represent an example of the approach in crystal engineering to modify the properties of a given structural model by means of isomorphous replacement; that is, replacement between Eu and Nd atoms can tune the optical property of the crystal while retaining the same structural model.

Conclusion

In summary, two major subjects were elaborated in this article: (a) Three isomorphous series of 3D hydrogen-bonded coordination frameworks have been assembled from the analogous [Ln(ntb)$(NO_3)_3$] monomers containing both HB donors and acceptors. Different N−H···O and O−H···O hydrogen-bonding fashions formed during crystallization in different solvent systems lead to three types of polymorphous crystals which display different porosities, while different lanthanide ions in isomorphs cause different luminescence. (b) The hydrogen-bonded coordination frameworks feature high thermal stability and framework robustness against guest removal, proven by single-crystal-to-single-crystal de/rehydration of the **2-Gd·2H$_2$O** complex. A study of gas and vapor adsorption/desorption behaviors of N_2, CO_2, H_2, and MeOH reveals a moderate storage capacity of CO_2, H_2, and MeOH and a selectivity of CO_2/N_2. A solvent adsorption investigation discloses the separation ability of a porous **2-Gd** framework for benzene over its derivatives.

Experimental Section

Physical Methods. Solvents and starting materials were purchased commercially and used without further purification unless otherwise noted. Lanthanide(III) nitrate was prepared by dissolving lanthanide oxide (99.99%) in 98% nitrate acid.[20] The ligand tris(2-benzimidazolylmethyl)amine (ntb) was synthesized following a slight modification of the method of Phillips by Oki et al.[21] to afford the product. Yield: *ca.* 72%. Infrared spectra were measured on a Nicolet/Nexus-670 FT-IR spectrometer with KBr pellets. The X-ray powder diffraction was recorded on a Rigaku D/Max-2200 diffractometer at 40 kV and 40 mA with a Cu-target tube and a graphite monochromator. Thermogravimetric analyses (TGA) were performed in the air under 1 atm at a heating rate of 10 °C/min^{-1} on a Perkin-Elmer/TGS-2 analyzer. Emission spectra were obtained on a Combined Fluorescence Lifetime and Steady State Spectrometer—FLS920. The adsorption isotherms for MeOH were measured in IGA-003 series, Hiden Isochema, Ltd. The adsorption isotherms of CO_2 were measured by using BELmax 00027 adsorption equipment (BEL Japan). The high-pressure hydrogen storage capability was evaluated at 77 K using a RUBOTHERM magnetic suspension balance (Ankersmid B.V., Netherlands). Before the measurements, the samples were evacuated under a dynamic vacuum at 120 °C for 24 h to remove the included solvent molecules.

Series 1: Complex 1-Gd·2H$_2$O and 1-Yb·2H$_2$O. A solution of ntb (40 mg, 0.1 mmol) in 2 mL of hot methanol and lanthanide nitrates (0.1 mmol) in 2 mL of methanol were carefully mixed. After cooling to room temperature and filtration, slow diffusion of ethyl ether into the mixture over three days afforded colorless crystals. Anal. Calcd for hydrated **1-Gd·2H$_2$O**, $GdC_{24}H_{25}N_{10}O_{11}$: C, 36.64; H, 3.20; N, 17.80. Found: C, 36.23; H, 3.92; N, 16.84. IR (KBr, ν/cm^{-1}): 3450(w), 3089(w), 2103(w), 1623(m), 1606(m),

(19) (a) Pan, M.; Zhang, X.-L.; Liu, Y.; Liu, W.-S.; Su, C.-Y. *Dalton Trans.* **2009**, 2157. (b) Judd, B. R. *J. Chem. Phys.* **1979**, *70*, 4830.

(20) Desreux, J. F. *Lanthanide Probes in Life, Chemical and Earth Sciences*; Choppin, G. R., Bünzli, J.-C. G., Eds.; Elsevier Publishing Co.: Amsterdam, 1989; Chapter 2, p 43.

(21) Oki, A. R.; Bommarreddy, P. K.; Zhang, H. M.; Hosmane, N. *Inorg. Chim. Acta* **1995**, *231*, 109.

1529(w), 1491(w), 1218(s), 1009(w), 807(w), 624(m), 658(w). Anal. Calcd for hydrated **1-Yb·2H$_2$O**, $YbC_{24}H_{25}N_{10}O_{11}$: C, 35.92; H, 3.14; N, 17.45%. Found, C, 35.26; H, 3.77; N, 16.86%. IR (KBr, ν/cm^{-1}): 3465(w), 3087(w), 2106(w), 1619(m), 1604(w), 1493(w), 1216(s), 1007(w), 811(w), 621(m), 655(w) cm^{-1}.

Series 2: 2-Eu, 2-Gd·2H$_2$O, 2-Er·H$_2$O, and 2-Nd·3H$_2$O. A solution of ntb (40 mg, 0.1 mmol) in 2 mL of hot methanol and lanthanide nitrates (0.1 mmol) in 2 mL of methanol were mixed carefully. A precipitate was formed and dissolved with 2 mL of DMF by constant heating. After cooling to room temperature and filtration, colorless single crystals were obtained by diffusion of ethylether within a week. Anal. Calcd for dehydrated **2-Eu**, $EuC_{24}H_{21}N_{10}O_9$: C, 38.66; H, 2.84; N, 18.79. Found: C, 36.71; H, 3.84; N, 16.95. IR (KBr, ν/cm^{-1}): 3088(w), 2103(w), 1621(m), 1602(m), 1529(w), 1491(w), 1218(s), 1010(w), 807(w), 624(m), 656(w). **2-Gd·2H$_2$O**, $GdC_{24}H_{25}N_{10}O_{11}$: C, 36.64; H, 3.20; N, 17.80. Found: C, 36.47; H, 3.05; N, 17.78. IR (KBr, ν/cm^{-1}): 3450(w), 3087(w), 2106(w), 1623(m), 1604(m), 1528(w), 1491(w), 1218(s), 1007(w), 811(w), 625(m), 656(w). **2-Er·H$_2$O**, $ErC_{24}H_{23}N_{10}O_{10}$: C, 37.01; H, 2.98; N, 17.99 1. Found: C, 36.73; H, 3.27; N, 17.39. IR (KBr, ν/cm^{-1}): 3465(w), 3087(w), 2101(w), 1620(m), 1601(m), 1528(w), 1493(w), 1216(s), 1007(w), 807(w), 624(m), 657(w). **2-Nd·3H$_2$O**, $NdC_{24}H_{27}N_{10}O_{12}$: C, 36.41; H, 3.44; N, 17.69. Found: C, 36.86; H, 3.58; N, 17.32. IR (KBr, ν/cm^{-1}): 3460(w), 3084(w), 2107(w), 1620(m), 1598(m), 1527(w), 1493(w), 1216(s), 1007(w), 811(w), 621(m), 655(w).

Serial 3: 3-Gd·1.5CH$_3$OH and 3-Er·1.5CH$_3$OH. A solution of ntb (20 mg, 0.05 mmol) in 2 mL of hot methanol and lanthanide nitrates (0.05 mmol) in 2 mL of methanol were mixed together. A precipitate was formed and dissolved by the addition of 1 mL of DMF and constant heating. After cooling to room temperature and filtration, colorless single crystals were obtained through the diffusion of ethylether within one week. Anal. Calcd for hydrated **3-Gd·1.5CH$_3$OH**, $Gd_2C_{51}H_{54}N_{20}O_{21}$: C, 38.34; H, 3.41; N, 17.53. Found: C, 37.93; H, 3.92; N, 17.64. IR (KBr, ν/cm^{-1}): 3468(w), 3089(w), 2102(w), 1617(m), 1606(m), 1529(w), 1493(w), 1218(s), 1009(w), 805(w), 624(m) and 655(w). Anal. Calcd for hydrated **3-Er·1.5CH$_3$OH**, $Er_2C_{51}H_{54}N_{20}O_{21}$: C, 37.87; H, 3.36; N, 17.32%. Found: C, 37.26; H, 3.77; N, 16.96%. IR (KBr, ν/cm^{-1}): 3465(w), 3084(w), 2107(w), 1621(m), 1604(m), 1527(w), 1493(w), 1216(s), 1007(w), 811(w), 621(m), 658(w).

Crystal Structure Determination. X-ray diffraction intensity data were collected on an Enraf-Nonius CAD4 diffractometer (Mo Kα radiation, λ = 0.71073 Å) for **2-Eu** and **2-Nd·3H$_2$O** at 293 K; on a Bruker SMART Apex CCD system with graphite-monochromated Mo Kα radiation (λ = 0.71073 Å) for **1-Yb·2H$_2$O** at 293 K; and on an Oxford Gemini S Ultra CCD system with graphite-monochromated Mo Kα radiation (λ = 0.71073 Å) for **2-Er·H$_2$O**, **3-Gd·1.5CH$_3$OH**, and **3-Er·1.5CH$_3$OH**, except **1-Gd·2H$_2$O** with Cu Kα radiation (λ = 1.54178 Å) at 293 K. Structures were solved by direct methods, followed by difference Fourier syntheses, and then were refined by full-matrix least-squares refinement on F^2 using SHELXL.[22] All of the non-hydrogen atoms were refined with anisotropic parameters, while H atoms were placed in calculated positions and refined using a riding model. The H atoms on the solvated water molecules were not added. For the **2-Gd·2H$_2$O** complex, variable-temperature single-crystal X-ray diffraction analyses were performed with the same crystal. The intensity data were recorded on an Oxford Gemini S Ultra CCD diffractometer with graphite-monochromated Mo Kα radiation (λ = 0.71073 Å). The data collection[23] was started first at 293 K for a fresh crystal (**2-Gd·2H$_2$O**), and then heated to 473 K (**2-Gd** (473 K)), and finally decreased to 293 K (**2-Gd·H$_2$O** (473 K-air)). The crystallinity of the sample was kept well during the temperature cycle, and the structures were refined satisfactorily. Crystallographic data and refinement parameters are listed in Tables S1 and S2 (Supporting Information). The selected bond distances and angles are listed in Tables S3 and S4 (Supporting Information). These data can be obtained free of charge from The Cambridge Crystallographic Data Centre via www.ccdc.cam.ac.uk/data_request/cif. The CCDC reference numbers are 767088−767097.

Acknowledgment. This work was supported by the 973 Program of China (2007CB815302) and the NSFC Projects (20903120, 20773167, 20731005, and U0934003).

Supporting Information Available: X-ray crystallographic data (CIF format), selected bond lengths and bond angles, additional crystal structure figures, XRD patterns and TGA curves. This material is available free of charge via the Internet at http://pubs.acs.org.

(22) Sheldrick, G. M. *SHELX 97*; Göttingen University: Göttingen, Germany, 1997.

(23) *CrysAlis CCD*; *CrysAlis RED*, version 1.171.31.7; Oxford Diffraction Ltd.: Oxford, U. K., 2006.